Korean J Physiol Pharmacol
Vol 7: 317–323, December, 2003

Electrophysiological and Morphological Classification of Inhibitory Interneurons in Layer II/III of the Rat Visual Cortex

Duck-Joo Rhie, Ho Young Kang, Gyeong Ryul Ryu, Myung-Jun Kim, Shin Hee Yoon, Sang June Hahn, Do Sik Min, Yang-Hyeok Jo, and Myung-Suk Kim

Department of Physiology, College of Medicine, The Catholic University of Korea, Seoul 137–701, Korea

Interneuron diversity is one of the key factors to hinder understanding the mechanism of cortical neural network functions even with their important roles. We characterized inhibitory interneurons in layer II/III of the rat primary visual cortex, using patch-clamp recording and confocal reconstruction, and classified inhibitory interneurons into fast spiking (FS), late spiking (LS), burst spiking (BS), and regular spiking non-pyramidal (RSNP) neurons according to their electrophysiological characteristics. Global parameters to identify inhibitory interneurons were resting membrane potential (> -70 mV) and action potential (AP) width (<0.9 msec at half amplitude). FS could be differentiated from LS, based on smaller amplitude of the AP ($< \sim 50$ mV) and shorter peak-to-trough time (P-T time) of the afterhyperpolarization (<4 msec). In addition to the shorter AP width, RSNP had the higher input resistance (>200 MΩ) and the shorter P-T time (<20 msec) than those of regular spiking pyramidal neurons. Confocal reconstruction of recorded cells revealed characteristic morphology of each subtype of inhibitory interneurons. Thus, our results provide at least four subtypes of inhibitory interneurons in layer II/III of the rat primary visual cortex and a classification scheme of inhibitory interneurons.

Key Words: Inhibitory interneurons, Classification, Visual cortex, Layer II/III

INTRODUCTION

The neuronal and synaptic organization of the cerebral cortex appears to be exceedingly complex, and the definition of a basic cortical circuit in terms of defined classes of cells and connections is necessary to facilitate the progress of its analysis. The cerebral cortex consists of: (i) a large population of principal neurons reciprocally connected to the thalamus and to each other via axon collaterals releasing excitatory amino acids, and (ii) a smaller population of mainly local circuit GABAergic neurons (Somogyi et al, 1998). Whereas the principal neurons are relatively homogeneous according to their regions, inhibitory interneurons consist of about 20 subtypes according to their morphological, electrophysiological, and neurochemical characteristics (Douglas & Martin, 1998). This interneuron diversity has hampered understanding of the nature of cortical neural network, although many important roles of the interneuron have recently been recognized, including synaptic plasticity, developmental change, synchronization of neuronal activity, and epilepsies. Thus, classification of the interneuron subtypes are crucial in interneuron research (Mott & Dingledine, 2003).

Organization of GABAergic interneurons and synapses has been relatively well studied in the hippocampus, because of its well layered structure and segregated location of inhibitory interneurons (Freund & Buzsaki, 1996). On the other hand, this is less apparent in the neocortex due to the complex lamination and intrinsic connections (Somogyi et al, 1998). Furthermore, no classification scheme of inhibitory interneurons has yet proved entirely satisfactory (McBain & Fisahn, 2001; Mott & Dingledine, 2003), because of the regional differences and different classification schemes among laboratories as well as their innate diversity. Classifications of inhibitory interneurons in the frontal cortex (Kawaguchi, 1995) and the somatosensory cortex (Gupta et al, 2000) have been reported. Although classification of cat primary visual cortical neurons with intracellular recording *in vivo* and staining was recently reported (Nowak et al, 2003), the authors found only one subtype of inhibitory interneurons. This might have been due to technical limitation of intracellular recording to secure a small population of inhibitory interneurons with small soma. Inhibitory interneurons in the visual cortex appear to be involved in the long-term synaptic plasticity, developmental change of synaptic connection between neurons and many visual functions (Sillito, 1979; Singer, 1995; Rozas et al, 2001). However, classification of inhibitory interneurons in the visual cortex has not yet been reported. Thus, in this study, we classified inhibitory interneurons in the layer II/III of the rat visual

Corresponding to: Duck-Joo Rhie, Department of Physiology, College of Medicine, The Catholic University of Korea, 505 Banpo-dong, Socho-gu, Seoul 137-701, Korea. (Tel) +82-2-590-1174, (Fax) +82-2-532-9575, (E-mail) djrhie@cmc.cuk.ac.kr

ABBREVIATIONS: Pyr, pyramidal neuron; FS, fast spiking neuron; LS, late spiking neuron; BS, burst spiking neuron; RSNP, regular spiking non-pyramidal neuron; RMP, resting membrane potential; P-T time, peak-to-trough time.

cortex electrophysiologically and morphologically with patch-clamp method using infrared-differential interference contrast (IR-DIC) video-microscopy, with which we could visually identify inhibitory interneurons. We also reconstructed biocytin-labeled recorded cells with confocal microscopy. Furthermore, we attempted to find quantitative parameters and a scheme to classify inhibitory interneurons into subtypes.

METHODS

Slice preparation

Coronal slices of visual cortex were prepared from rats at postnatal day 21~30. Animals were anesthetized with chloral hydrate (400 mg/kg, i.p.; Merck, Germany) and decapitated. The brains were quickly isolated and submerged in ice-cold physiological Ringer's solution. Coronal sections of occipital cortex (300 μm thick) were made on a vibroslicer and allowed to recover in a submerged slice chamber for 30 min at 37°C. Slices were maintained at room temperature prior to recording. Dissection and storing medium consisted of 125 mM NaCl, 2.5 mM KCl, 1 mM $CaCl_2$, 2 mM $MgSO_4$, 1.25 mM KH_2PO_4, 25 mM $NaHCO_3$, and 10 mM D-glucose, bubbled with 95% O_2 and 5% CO_2. The slices were transferred to the recording chamber and superfused continuously with artificial cerebrospinal fluid (1.5~2 ml/min) containing 125 mM NaCl, 2.5 mM KCl, 2 mM $CaCl_2$, 1 mM $MgSO_4$, 1.25 mM KH_2PO_4, 25 mM $NaHCO_3$, and 10 mM D-glucose, bubbled with 95% O_2 and 5% CO_2. All recordings were performed at 32~33°C.

Whole-cell patch clamping and electrical stimulation

Standard whole-cell patch clamp technique with a bridge amplifier (IX2-700, Dagan, USA) was used to record membrane potential and synaptic events. The patch electrodes (4~8 MΩ) were filled with a pipette solution containing 130 mM K gluconate, 10 mM KCl, 3 mM MgATP, 10 mM phosphocreatine, 0.3 mM GTP, 10 mM HEPES, 0.2 mM EGTA, and 50 U/ml creatine phosphokinase (pH adjusted to 7.25 with KOH). We added biocytin (0.5%; Sigma, USA) to the pipette solution to reconstruct the recorded cells. Under visual guidance, utilizing IR-DIC video-microscopy on an upright microscope (BX50-WI fitted with 40×/0.80NA water immersion objective, Olympus, Japan), potential interneurons in the layer II/III of the primary visual cortex were distinguished from pyramidal neurons (Pyr), according to their bipolar or multipolar dendritic processes as well as their bipolar, oval, or round somata. Negative pressure was applied to the patch electrode to obtain a seal of more than 2 GΩ. Whole-cell configuration was obtained with applying brief negative air pressure.

Passive membrane characteristics were obtained with 300-msec step pulse of negative current evoking about -10 mV deflection. Action potentials (APs) were evoked with positive step current injection with graded increment of 10 or 20 pA. Orthodromic synaptic responses were elicited by stimulating two sets of afferents with concentric bipolar tungsten electrodes (100 μm in diameter). One electrode was placed below the recorded cell in layer IV (vertical pathway) and the other lateral in layer II (horizontal pathway). Synaptic responses were evoked with a pair of two pulses (0.1 msec) with interstimulus interval of 50 msec, repeated every 10 sec. Stimulus intensity was adjusted to induce the first excitatory postsynaptic potential (EPSP) amplitudes in the range of 3~7 mV. Synaptic responses were evoked at resting membrane potential (RMP). Command generation, data collection and analysis were performed with pClamp 8.0 or 9.0 suite (Axon Instruments, USA). Data were filtered at 4 kHz, sampled at 20 kHz, and stored in a Pentium PC.

Staining and confocal reconstruction

The slices were fixed overnight at 4°C with 4% paraformaldehyde in 0.1 M sodium phosphate buffer (pH 7.4) following the recording. After several washes with 0.01 M sodium phosphate-buffered saline (PBS), the slices were incubated overnight at 4°C with 0.5% Triton X-100 in PBS to permeabilize cell membranes. Subsequently, the slices were reacted for 1 h at room temperature with fluorescein-conjugated avidin (1 μg/ml in PBS, Alexa Fluor 488, Molecular Probes, USA) to detect intracellular biocytin. The slices were rinsed and mounted with glycerol gelatin (Merck) on glass slides. Then, the distribution of intracellular biocytin was reconstructed under confocal microscopy (MRC1024, Bio-Rad Laboratories, USA).

Statistical analysis

All data were expressed as mean±S.E. Analysis of variance (ANOVA) was used for the statistical comparison. A *P*-value of less than 0.05 was considered statistically significant.

RESULTS

We analyzed 42 neurons recorded from layer II/III of the rat primary visual cortex. Of them, 10 neurons were Pyr, and 32 neurons were non-pyramidal inhibitory interneurons. According to their passive and active electrophysiological characteristics, inhibitory interneurons were classified into fast spiking (FS), late spiking (LS), burst spiking (BS), and regular spiking non-pyramidal (RSNP) neurons. The cells recorded were morphologically characterized with biocytin staining.

Passive membrane properties

RMP and input resistance (IR) of Pyr were −78.6±1.1 mV and 120±12 MΩ (n=10), respectively, which were not different from other report (Tamas et al, 2002) (Table 1). RMP of the inhibitory interneurons was invariably more depolarized than that of Pyr, and RMP of RSNP (−60.5±1.3 mV, n=9) was even higher than that of BS (−70.3±2.1 mV, n=7). IR of RSNP (345±25 MΩ) was higher than that of Pyr or FS (141±16 MΩ, n=7). Relaxation time constants (tau) of hyperpolarizing membrane response in FS, LS and BS were lower than that of Pyr or RSNP. In general, interneurons had higher IR and faster time constant than Pyr. RSNP showed particularly higher IR than that of Pyr. These electrical properties might favor fast membrane response and spike generation in response to inward synaptic current.

Table 1. Passive membrane properties of pyramidal neurons and inhibitory interneurons

	Pyr (10)	FS (7)	LS (9)	BS (7)	RSNP (9)
RMP	−78.6±1.1	−66.4±2.4[a]	−66.3±1.8[a]	−70.3±2.1[a]	−60.5±1.3[ad]
IR	120±12	141±16	185±23[e]	222±18[ae]	346±25[ab]
τ	21.6±1.2	7.5±0.7[a]	13.0±1.3[ae]	13.8±1.8[abe]	22.2±1.5[b]

IR and τ were measured with hyperpolarization response of about −5~−15 mV from RMP by negative step current injection into the soma (40~50 pA, 300 msec). a: vs. Pyr, $P<0.05$; b: vs. FS, $P<0.05$; d: vs. BS, $P<0.05$; e: vs. RSNP, $P<0.05$.

Table 2. Active membrane properties of pyramidal neurons and inhibitory interneurons

	Pyr (10)	FS (7)	LS (9)	BS (7)	RSNP (9)
AP threshold (mV)	−36.1±1.8	−32.3±2.4	−33.2±1.3	−39.3±0.6	−35.2±1.4
AP amplitude[1] (mV)	76.6±2.9	42.6±3.9[a]	60.8±2.7[ab]	53.9±2.9[a]	61.0±2.8[ab]
AP width[2] (msec)	1.32±0.07	0.62±0.05[a]	0.74±0.03[a]	0.84±0.14[a]	0.60±0.04[a]
AHP[3] (mV)	−14.3±1.3	−17.3±1.5	−23.5±1.1[ab]	−6.3±1.4[abc]	−13.0±0.9[cd]
P-T time[4] (msec)	44.2±4.8	2.8±0.5[a]	6.9±0.8[a]	3.1±1.3[a]	11.6±2.7[a]
AP adaptation[5]	1.26±0.10[c]	1.04±0.02	0.99±0.01	−	1.29±0.10[c]

AP was generated with step current injection of 10~20 pA for 980 msec. All the parameters except AP adaptation were measured at the first AP evoked by minimal current amplitude. 1: AP amplitude was measured from AP threshold to the peak level. 2: AP width was measured at half amplitude of AP. 3: Afterhyperpolarization (AHP) was measured from AP threshold to the trough peak of the AHP. 4: P-T time was measured from AP peak to trough peak. 5: AP adaptation was calculated with average of inter-spike interval of fifth and sixth APs divided by inter-spike interval of third and fourth APs, when at least six consecutive APs were generated with minimum current injection. a: vs. Pyr, $P<0.05$; b: vs. FS, $P<0.05$; c: vs. LS, $P<0.05$; d: vs. BS, $P<0.05$.

Table 3. Synaptic response of pyramidal neuron and inhibitory interneurons

	Pyr (10)	FS (6)	LS (9)	BS (7)	RSNP (7)
Vertical input peak time	8.8±0.7	7.8±1.2	5.7±0.5	7.4±0.6	8.7±1.4
Vertical input PPR	1.11±0.13	1.06±0.16	1.09±0.17	0.93±0.20	1.47±0.28
Horizontal input peak time	10.7±0.7	7.6±0.4	7.5±0.8[a]	9.7±0.5	10.2±1.3
Horizontal input PPR	1.15±0.13	1.24±0.22	0.97±0.11	1.00±0.15	1.37±0.21

Synaptic activation was evoked by extracellular stimulation of 0.1 msec duration, which induced about 5 mV EPSP. Peak time was calculated from the stimulus artifact to time at peak of the EPSP. PPR was calculated with dividing amplitude of 2nd EPSP by that of 1st EPSP from RMP. a: vs. Pyr, $P<0.05$

Active membrane properties

Most striking difference of AP generation in response to positive step current injection between Pyr and inhibitory interneurons was the duration and the amplitude of the APs (Table 2). Whereas AP width of the Pyr was 1.32±0.07 msec, that of all interneurons was less than 0.9 msec. This result was in accordance with other report in the hippocampus (Erisir et al, 1999) and the frontal cortex (Kawaguchi & Kubota, 1996). However, there was no difference in AP width among four subtypes of the interneurons. Peak-to-trough (P-T) time was also a good parameter to distinguish RSNP (11.6±2.7 msec) from Pyr (44.2±4.8 msec). LS cells were previously reported to be in layer II/III of the frontal cortex (Kawaguchi & Kubota, 1996), layer I of the somatosensory and visual cortex (Chu et al, 2003), and layer VI of the perirhinal cortex (McGann et al, 2001). In this study, LS cells were frequently found in layer II/III of the primary visual cortex. These cells have often been confused with FS cells. According to our analysis, however, they could clearly be distinguished from FS, based on AP amplitude and P-T time. AP width and P-T time are also good parameters for differentiation of RSNP from Pyr. AP adaptation, which has been shown in Pyr and RSNP, was not observed in FS and LS.

Synaptic response

To examine short-term kinetics of synaptic activities among inhibitory interneurons (Reyes et al, 1998; Losonczy et al, 2002), we evoked synaptic responses to extracellular stimulation in layer II and layer IV, which may represent the intracortical and thalamocortical inputs to layer II/III cells, respectively. There was no difference between interneuron subtypes in peak time and paired-pulse ratio (PPR) of EPSP in the vertical and horizontal inputs, except that LS showed faster peak time in the horizontal input than Pyr (Table 3).

Morphology

Confocal reconstruction of the recorded cells revealed different morphology, depending on electrophysiological subtypes of inhibitory interneurons (Fig. 1). Pyr showed

invariably typical pyramid-shaped soma, dendritic arbor of apical bifurcation, and fine basal dendrites with many dendritic spines. Main axon arose from the soma or one of the basal dendrites and went down to the layer V and VI. Many collaterals distributed their axon terminals in the layer II/III. On the other hand, inhibitory interneurons showed variable shapes, depending on subtypes. FS showed extensive axonal arbor around the soma within about 200 μm, as seen in Fig. 1. Dendrites were not reconstructed in this cell. Another FS cell showed multipolar short dendritic processes of about 50 μm in length (data not shown). LS exhibited multipolar dendritic processes within about 100 μm

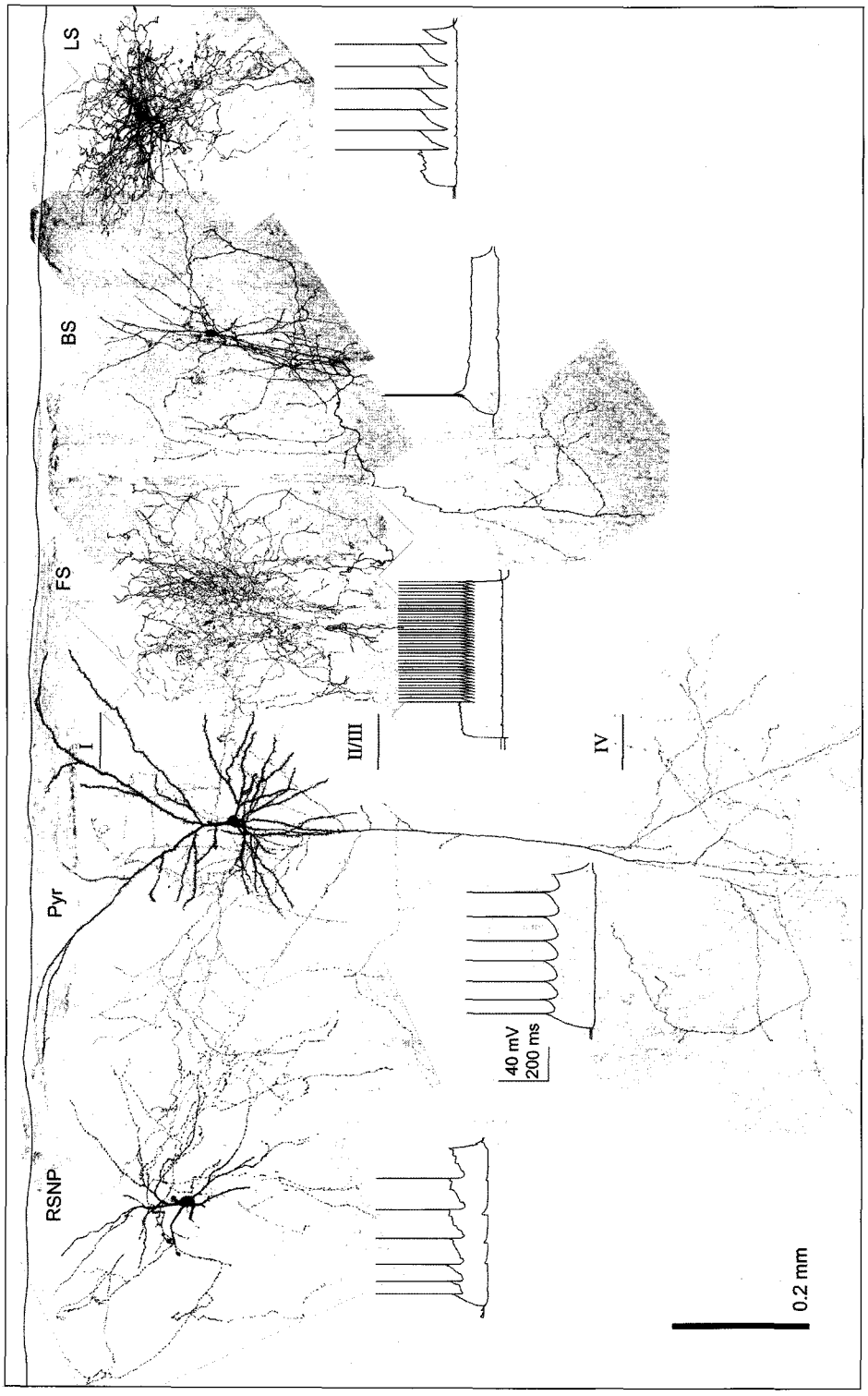

Fig. 1. Confocal reconstruction of recorded cells and their spiking patterns. Whereas Pyr showed dense dendritic spines on apical and basal dendrites, no dendritic spines were observed in all other inhibitory interneurons. Axonal arbors of interneurons were confined to layer II/III except BS. FS and LS extend extensive axonal trees around the soma. Representative APs were evoked by step current injection (160 pA, 360 pA, 140 pA, 80 pA, and 80 pA for Pyr, FS, LS, BS, and RSNP, respectively) and hyperpolarizing response were produced by −20 pA in all neurons. EPSPs recorded with extracellular stimulation are also shown.

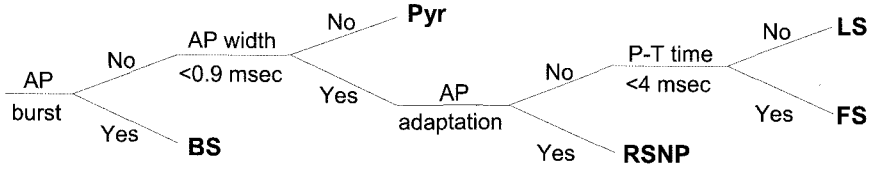

Fig. 2. Classification scheme of inhibitory interneurons in layer II/III of the visual cortex. Stepwise processes based on non-overlapping parameters were adopted for classification of various neuronal subtypes. Other parameters could be combined in this scheme to avoid possible errors in unusual cases (see the text).

from the soma and wider distribution of axonal arbor (n=8 of 9 cells). In contrast to apical dendrites of Pyr, dendritic and axonal trees of the both subtypes rarely invaded layer I and were confined in the supragranular layer (one exception in LS). BS showed vertically oriented bipolar shape of the soma and dendritic arbor (n=6 of 7 cells). Usually their axons ran vertically through layer IV to infragranular layer. RSNP had multiple initiations of main dendrites from the soma and sparsely distributed axonal trees in supragranular layer (n=8 of 9 cells). In general, dendrites and axons of inhibitory interneurons, except BS, were confined in layer II/III. Axons of a BS cell showed many terminals distributing in entire cortical column (data not shown). Taken together, our classification of inhibitory interneurons in the rat primary visual cortex, based on the electrophysiological characteristics, is well correlated with their morphological variability.

DISCUSSION

Classification scheme of inhibitory interneurons

To the best of our knowledge, this is the first report to classify inhibitory interneurons in the rat visual cortex. We grouped inhibitory interneurons according to their electrophysiological and morphological characteristics, and we clearly have found four main subtypes of inhibitory interneurons: FS, LS, BS and RSNP. Since they have many overlapping features with each other, we analyzed the electrophysiological parameters with stepwise procedures to find a classification scheme (Fig. 2). Inhibitory interneurons were clearly distinguished from regular spiking Pyr with two parameters: typically, Pyr generated adapting spike of longer AP width (>0.9 msec at half amplitude) and P-T time (>20 msec) with step depolarization than those of inhibitory interneurons. Two exceptions were noticed in BS, however, it was not difficult to identify them as inhibitory interneurons because of their bursting nature of spiking. RSNP could be recognized with AP adaptation at this step. FS and LS showed relatively similar pattern of spiking and have overlapping features. In this study, we found some good parameters to differentiate them: although there was only a narrow interval in P-T time between the two subtypes (4 msec), P-T time was an adequate classification parameter. Possible errors in differentiating RSNP from Pyr could be avoided by comparing other parameters such as IR and PT time (Table 1, 2). RMP does not seem to be an adequate parameter to identify interneurons, because damaged cell also is depolarized.

Although there are many electrophysiological parameters available in classifying inhibitory interneurons, some cells show atypical and equivocal behavior. This is partly due to unavoidable artificial factors during the slice preparation, because the spiking pattern is also dependent on the dendritic structure of the neuron (Mainen & Sejnowski, 1996). Within the subtypes, they also have different neurochemical properties (Freund & Buzsaki, 1996). Thus, morphological and neurochemical parameters are essential to classify them into more homogeneous subtypes. This interneuronal diversity may be related with diverse roles played by inhibitory interneurons (Buhl et al, 1998; Blatow et al, 2003).

Spiking pattern and subtype of inhibitory interneurons

Identification of neuronal subtypes is essential to facilitate studying the mechanism of the brain function. Since "fast spiking" and "regular spiking" cells were described in the monkey brain cortex (Mountcastle et al, 1969), other subtypes of excitatory and inhibitory neurons have been reported, according to their different neuronal properties such as laminar location, dendritic and axonal morphology, neurochemical properties, and intrinsic electrophysiological properties. Of these, intrinsic electrophysiological properties are of primary importance, because they strongly influence the input-output relationships and operation of cortical neurons and circuits (Nowak et al, 2003). There are discrepancies between our study and a recent report on *in vivo* identification of regular spiking, fast spiking, chattering, and intrinsically bursting cells in the cat visual cortex (Nowak et al, 2003). FS cells are recognized in most cortical areas with high frequency spiking and characteristic neurochemical properties (Kawaguchi, 1995; Freund & Buzsaki, 1996), and they seem to be very important in sensory perception with generating fast gamma rhythm (Buhl et al, 1998). In this study, LS generated slower spikes than FS and showed continuous build-up of depolarization with step current injection (Fig. 1). LS cells have been reported in various cortical areas (Kawaguchi, 1995; McGann et al, 2001; Chu et al, 2003). BS and RSNP were also reported in the frontal and somatosensory cortex (Kawaguchi, 1995; Gupta et al, 2000). In this study, we also identified four subtypes of inhibitory interneurons in the visual cortex. However, we found no chattering cells. Many variable factors such as species, age, environment, and experimental condition of the animal are involved in identifying neuronal subtypes with electrophysiological properties. Although *in vivo* recording seems to be the most

physiological to study electrophysiological properties of neurons, it is possible to miss many inhibitory interneurons of small population with small soma (Nowak et al, 2003). In spite of artificial condition of *in vitro* recording with slices, we clearly identified four subtypes of inhibitory interneurons with different electrophysiological properties and morphologies. Inhibitory interneurons in the visual cortex mature to the adult level by P30 (Miller, 1986; Parnavelas, 1992). In this study, we used rats aged 3rd and early 4th postnatal weeks, therefore, properties and proportion of inhibitory interneurons could be different from those of adult rats, which should to be studied.

At least three factors are involved in the spiking pattern of neurons: (i) dendritic structure (Mainen & Sejnowski, 1996), (ii) passive properties of the membrane and ion channels (Erisir et al, 1999; Sanchez-Vives et al, 2000; Rudy & McBain, 2001), and (iii) neurochemical properties of calcium binding proteins (Kawaguchi & Kubota, 1993). Adaptation of AP generation by step current injection in Pyr is dependent on the activation of sodium- and calcium-activated K channels (Sanchez-Vives et al, 2000). Fast activating Kv3.1 and Kv3.2 channels play an important role in fast spiking in FS (Rudy & McBain, 2001). Calcium binding proteins such as parvalbumin, calbindin, and calretinin are distributed differentially in inhibitory interneurons (Freund & Buzsaki, 1996), and differential distribution of these variables may be involved in the shaping of the spiking. Contribution of various ion channels on the spiking pattern in different subtypes of inhibitory interneurons remains to be studied.

Inhibitory interneuron and short-term synaptic plasticity

Synapses exhibit short-term plasticity patterns, and this behavior influences information processing in neuronal networks. Although the underlying mechanism of short-term synaptic plasticity mostly relies on the presynaptic calcium dynamics (Katz & Miledi, 1968), it has been suggested that it may depend on the identity of the postsynaptic target cell (Reyes et al, 1998; Scanziani et al, 1998; Losonczy et al, 2002). Furthermore, different PPR between multipolar bursting interneurons and pyramidal neurons has been reported (Blatow et al, 2003). However, in this study, we found no difference in PPR among inhibitory interneurons. This might be partly due to stimulation of multiple axons from heterogeneous neuronal population by extracellular stimulation. To overcome this technical limitation in further study, dual patch-clamping of connected pair seems to be necessary (Ali et al, 1998; Gupta et al, 2000; Losonczy et al, 2002).

We reported herein four subtypes of inhibitory interneurons in layer II/III of the rat visual cortex. Each subtype of inhibitory interneurons may play a specific role in cortical information processing. This study will facilitate to elucidate the underlying mechanism by which cortical neural network functions.

ACKNOWLEDGEMENT

This study was supported by a grant from the Korea Ministry of Health and Welfare (02-PJ1-PG3-21302-0012).

REFERENCES

Ali AB, Deuchars J, Pawelzik H, Thomson AM. CA1 pyramidal to basket and bistratified cell EPSPs: dual intracellular recordings in rat hippocampal slices. *J Physiol* 507: 201–217, 1998

Blatow M, Rozov A, Katona I, Hormuzdi SG, Meyer AH, Whittington MA, Caputi A, Monyer H. A novel network of multipolar bursting interneurons generates theta frequency oscillations in neocortex. *Neuron* 38: 805–817, 2003

Buhl EH, Tamas G, Fisahn A. Cholinergic activation and tonic excitation induce persistent gamma oscillations in mouse somatosensory cortex in vitro. *J Physiol* 513: 117–126, 1998

Chu Z, Galarreta M, Hestrin S. Synaptic interactions of late-spiking neocortical neurons in layer 1. *J Neurosci* 23: 96–102, 2003

Douglas R, Martin K. Neocortex. In: Shepherd GM. Ed, The synaptic organization of the brain. 4th ed, Oxford, New York, p 459–509, 1998

Erisir A, Lau D, Rudy B, Leonard CS. Function of specific K(+) channels in sustained high-frequency firing of fast-spiking neocortical interneurons. *J Neurophysiol* 82: 2476–2489, 1999

Freund TF, Buzsaki G. Interneurons of the hippocampus. *Hippocampus* 6: 347–470, 1996

Gupta A, Wang Y, Markram H. Organizing principles for a diversity of GABAergic interneurons and synapses in the neocortex. *Science* 287: 273–278, 2000

Katz B, Miledi R. The role of calcium in neuromuscular facilitation. *J Physiol* 195: 481–492, 1968

Kawaguchi Y. Physiological subgroups of nonpyramidal cells with specific morphological characteristics in layer II/III of rat frontal cortex. *J Neurosci* 15: 2638–2655, 1995

Kawaguchi Y, Kubota Y. Correlation of physiological subgroupings of nonpyramidal cells with parvalbumin- and calbindinD28k-immunoreactive neurons in layer V of rat frontal cortex. *J Neurophysiol* 70: 387–396, 1993

Kawaguchi Y, Kubota Y. Physiological and morphological identification of somatostatin- or vasoactive intestinal polypeptide-containing cells among GABAergic cell subtypes in rat frontal cortex. *J Neurosci* 16: 2701–2715, 1996

Losonczy A, Zhang L, Shigemoto R, Somogyi P, Nusser Z. Cell type dependence and variability in the short-term plasticity of EPSCs in identified mouse hippocampal interneurones. *J Physiol* 542: 193–210, 2002

Mainen ZF, Sejnowski TJ. Influence of dendritic structure on firing pattern in model neocortical neurons. *Nature* 382: 363–366, 1996

McBain CJ, Fisahn A. Interneurons unbound. *Nat Rev Neurosci* 2: 11–23, 2001

McGann JP, Moyer JR Jr, Brown TH. Predominance of late-spiking neurons in layer VI of rat perirhinal cortex. *J Neurosci* 21: 4969–4976, 2001

Miller MW. The migration and neurochemical differentiation of gamma-aminobutyric acid (GABA)-immunoreactive neurons in rat visual cortex as demonstrated by a combined immunocytochemical-autoradiographic technique. *Brain Res* 393: 41–46, 1986

Mott DD, Dingledine R. Interneuron Diversity series: Interneuron research--challenges and strategies. *Trends Neurosci* 26: 484–488, 2003

Mountcastle VB, Talbot WH, Sakata H, Hyvarinen J. Cortical neuronal mechanisms in flutter-vibration studied in unanesthetized monkeys. Neuronal periodicity and frequency discrimination. *J Neurophysiol* 32: 452–484, 1969

Nowak LG, Azouz R, Sanchez-Vives MV, Gray CM, McCormick DA. Electrophysiological classes of cat primary visual cortical neurons in vivo as revealed by quantitative analyses. *J Neurophysiol* 89: 1541–1566, 2003

Parnavelas JG. Development of GABA-containing neurons in the visual cortex. *Prog Brain Res* 90: 523–537, 1992

Reyes A, Lujan R, Rozov A, Burnashev N, Somogyi P, Sakmann

B. Target-cell-specific facilitation and depression in neocortical circuits. *Nat Neurosci* 1: 279–285, 1998

Rozas C, Frank H, Heynen AJ, Morales B, Bear MF, Kirkwood A. Developmental inhibitory gate controls the relay of activity to the superficial layers of the visual cortex. *J Neurosci* 21: 6791–6801, 2001

Rudy B, McBain CJ. Kv3 channels: voltage-gated K+ channels designed for high-frequency repetitive firing. *Trends Neurosci* 24: 517–526, 2001

Sanchez-Vives MV, Nowak LG, McCormick DA. Cellular mechanisms of long-lasting adaptation in visual cortical neurons in vitro. *J Neurosci* 20: 4286–4299, 2000

Scanziani M, Gahwiler BH, Charpak S. Target cell-specific modulation of transmitter release at terminals from a single axon. *Proc Natl Acad Sci USA* 95: 12004–12009, 1998

Sillito AM. Inhibitory mechanisms influencing complex cell orientation selectivity and their modification at high resting discharge levels. *J Physiol* 289: 33–53, 1979

Singer W. Development and plasticity of cortical processing architectures. *Science* 270: 758–764, 1995

Somogyi P, Tamas G, Lujan R, Buhl EH. Salient features of synaptic organisation in the cerebral cortex. *Brain Res Brain Res Rev* 26: 113–135, 1998

Tamas G, Szabadics J, Somogyi P. Cell type- and subcellular position-dependent summation of unitary postsynaptic potentials in neocortical neurons. *J Neurosci* 22: 740–747, 2002